Appendix 1

Maps and Spectra of Jupiter and the Galilean Satellites

J. R. Spencer
Lowell Observatory, Flagstaff AZ

R. W. Carlson
Jet Propulsion Laboratory, California Institute of Technology

T. L. Becker, J. S. Blue
U. S. Geological Survey, Flagstaff AZ

A1.1 SPECTRA

The spectra (Figs. A1.1–A1.3) cover separately the reflected sunlight (0.2–~5 μm) and thermal emission (>~5 μm) wavelength regions for Jupiter and the Galilean satellites, using a logarithmic wavelength scale to give all spectral regions comparable coverage. All spectra have been binned to a maximum resolution ($\lambda/\delta\lambda$) of ~1000. We have used the best available spectra in each wavelength regime, so different spectra may cover different parts of each body, and there is a mixture of disk-resolved and disk-integrated data.

An attempt has been made at rough absolute calibration, in units of geometric albedo (including the opposition effect for the satellites, consistent with the IAU convention (Bowell *et al.* 1989)) for the reflected regime and brightness temperature for the thermal emission regime. All satellite reflectance spectra are scaled to match ground-based multi-wavelength geometric albedo measurements (Morrison and Morrison (1977) for u, v, b, and V, and Tittemore and Sinton (1989) for K, L′, and M), shown by horizontal gray bars.

Letters label specific spectral features, though the weaker features are not always obvious in the spectra as reproduced here. In the interest of simplicity we do not give citations for the discovery or identification of these features: see the rest of the book for details. For the icy satellite spectra, unlabelled features are due to H_2O ice, and the other spectral features have consistent labels as follows: A = SO_2; B = O_2; C = bound H_2O; D = H_2O_2; E = CO_2; F = O_3; G = C–H (?); H = S–H (?); I = C–N (?); J = O–H or bound H_2O (where the question marks indicate some uncertainty in the identification of spectral features). For the other bodies, spectral identifications are given in the captions. For the satellites, the letter in square brackets next to the spectrum label refers to the satellite hemisphere observed: L = leading; T = trailing; A = anti-Jupiter; J = Jupiter-facing.

A1.2 MAPS

The Jupiter "map" (Fig. A1.8 and Plate 16) shows cloud features as imaged by the *Cassini* ISS camera on October 31, 2002, using a simple rectangular projection of planetocentric coordinates. The longitude scale is System II, in which mid-latitude cloud features are relatively static. System III longitude values were 38° smaller on this date. Two latitude systems are shown: planetocentric latitude θ_C and planetographic latitude θ_G: these are related by the formula $\tan(\theta_C) = O^2 \tan(\theta_G)$, where O is the ratio of Jupiter's polar diameter to its equatorial diameter, 0.9352. A *Voyager*-based zonal (east/west) wind profile, from Limaye (1986) is shown: the *Cassini* wind profile (Porco *et al.* 2003) is very similar. The wind profile defines the classical "belts" and "zones", as shown: belts have cyclonic latitudinal wind shear and zones have anticyclonic shear. Zones tend to be covered in high-altitude, high-albedo cloud and are thus generally lighter in color than belts. Belt/zone boundaries and classical nomenclature are from Rogers (1995): NNTB = North north temperate belt; NTZ = North temperate zone; NTB = North temperate belt; NTrZ = North tropical zone; NEB = North equatorial belt; EZ = Equatorial zone; and similarly for the southern hemisphere. The two largest long-lived cloud features are the Great Red Spot, at longitude 75° latitude −20° (planetocentric) at this epoch, and White Oval AE at longitude 285°, latitude −30° (planetocentric).

We provide two Io maps, one in color (Fig. A1.8 and Plate 16) to show color and albedo patterns, and one in grayscale (Fig.) to show topography. The enhanced-color map was made using a simple rectangular projection, showing major albedo features and selected volcanoes. The base map is from Geissler *et al.* (1999), and uses *Galileo* images taken in 1996 and 1997 at 0.41, 0.56, and 0.76 μm, at low phase angles (0.5–13.9°). The grayscale Io map is a custom map (estimated accuracy of location of features ~10–20 km). The icy Galilean satellite maps (Figs. –) are compact versions of new U. S. Geological Survey (USGS) photomosaic maps incorporating the best regional *Voyager* and *Galileo* imagery, and new control networks developed by the USGS. Modifications for this appendix include enlargement of labels for readability, and removal of some feature names to avoid crowding. Full-sized paper versions of the icy satellite maps are available from the USGS (map numbers

I-2757, I-2770, and I-2762 for Europa, Ganymede, and Callisto repectively), with Io to follow soon, and are available electronically (see accompanying CD or www.astrogeology.usgs.gov). For all the grayscale maps, Mercator projection is used for low latitudes and polar stereographic projection for high latitudes. Maps are for positional reference only and are not intended to be photometrically accurate.

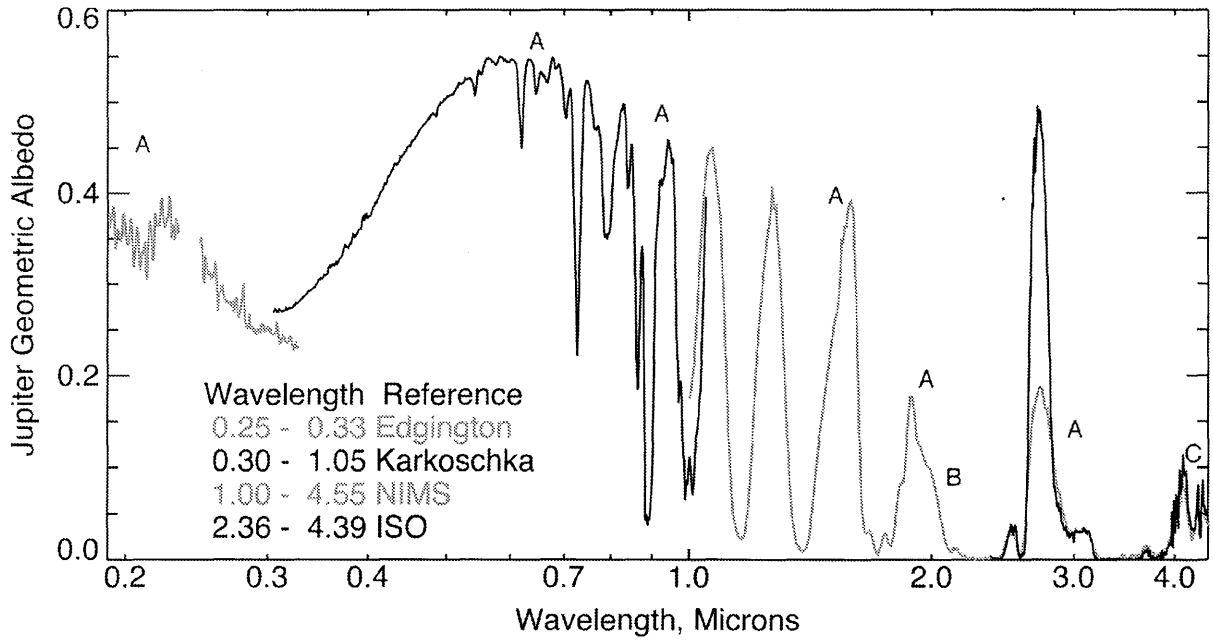

Figure A1.1. Jupiter reflectance spectrum. A = NH_3; B = H_2; C = PH_3. Other features are due to CH_4, though most fine structure in the UV spectrum is noise. References: Edgington *et al.* (1998), Edgington *et al.* (1999), Karkoschka (1998); NIMS: Carlson *et al.* (1996); ISO: Encrenaz *et al.* (1996), Encrenaz *et al.* (1999). The ISO flux spectrum is divided by a 6000 K blackbody to convert to albedo.

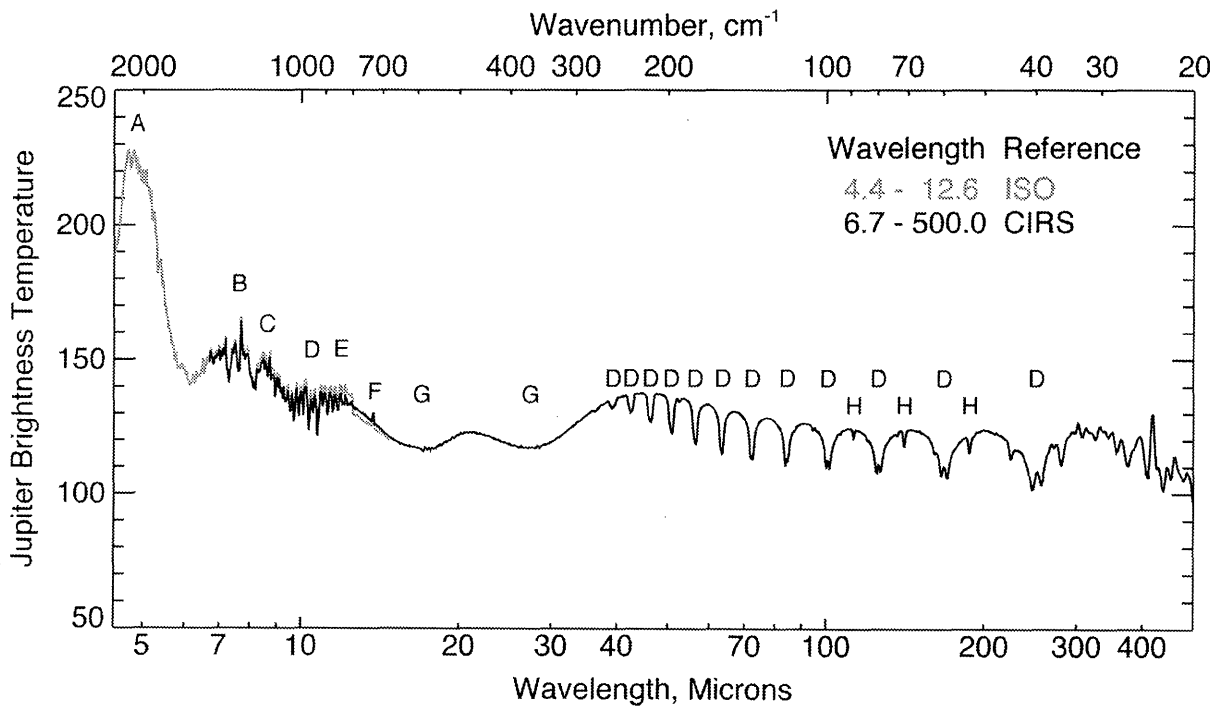

Figure A1.2. Jupiter emission spectrum. A = numerous species including H_2O, PH_3, GeH_4, NH_3, CO; D = NH_3; E = C_2H_6; F = C_2H_2, G = H_2; H = PH_3. References: ISO: Encrenaz *et al.* (1996), Encrenaz *et al.* (1999); CIRS: Hanel *et al.* (2003).

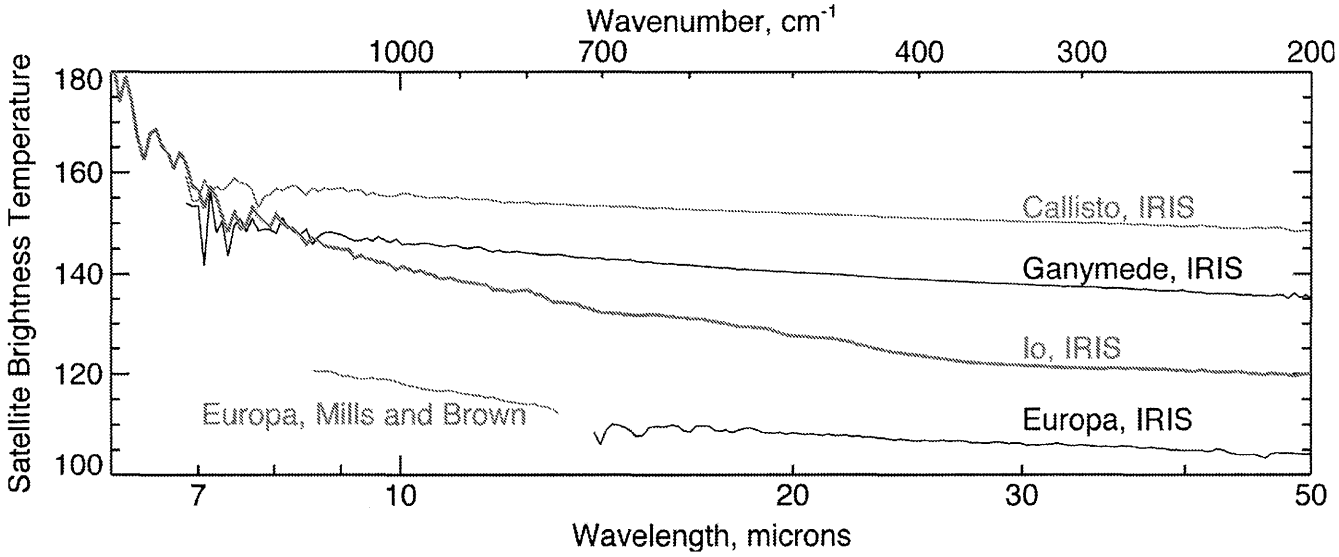

Figure A1.3. Galilean satellite emission spectra, binned to a spectral resolution of 94 to reduce noise, mostly obtained by the *Voyager* Infrared Interferometer Spectrometer (IRIS) (Spencer 1987). The fine structure at short wavelengths is probably noise. Note: the IRIS spectra of the icy satellites are disk-resolved, the Io spectrum is disk-integrated. Io's spectrum has steeper slope and broad features, in contrast to the featureless and more nearly blackbody emission from the icy satellites. *Io*: mean of 13 *Voyager 1* IRIS full-disk spectra. Io fills roughly 90% of the field of view, brightness temperatures being corrected for this filling factor. The volcanic component accounts for the steep rise in brightness temperature at shorter wavelengths. Broad, shallow, spectral features in the 10–30 μm region may come from surface SO_3 (Khanna *et al.* 1995). FDS count range 16 368.25–16 368.49; phase angle = 15°; sub-spacecraft point at 156° W, 0° N. *Europa 14–50 μm*: Mean of 6 warmest on-disk *Voyager 2* IRIS resolved spectra (substantially colder than the unobserved subsolar region). FDS count range 20 649.44–20 650.47; mean location 163° W, 10° S; phase angle = 92°; emission angle = 34°; local time = 4 pm. *Europa 8.5–13.3 μm*: Ground-based Europa spectrum, scaled to Callisto, from Mills and Brown (2000). *Ganymede*: Mean of 7 warmest *Voyager 1* IRIS disk-resolved spectra, covering Nicholson Regio. FDS count range = 16 402.21–16 402.29, mean location = 0° W, 15° S, phase angle = 50°, emission angle = 30°, local time = 2 pm. *Callisto*: Mean of 6 warmest *Voyager 1* IRIS resolved spectra, covering a region SE of Valhalla. FDS count range 16 418.29–16 418.34, mean location = 13° W, 0° N, phase angle = 41°, emission angle = 20°, local time = 2 pm.

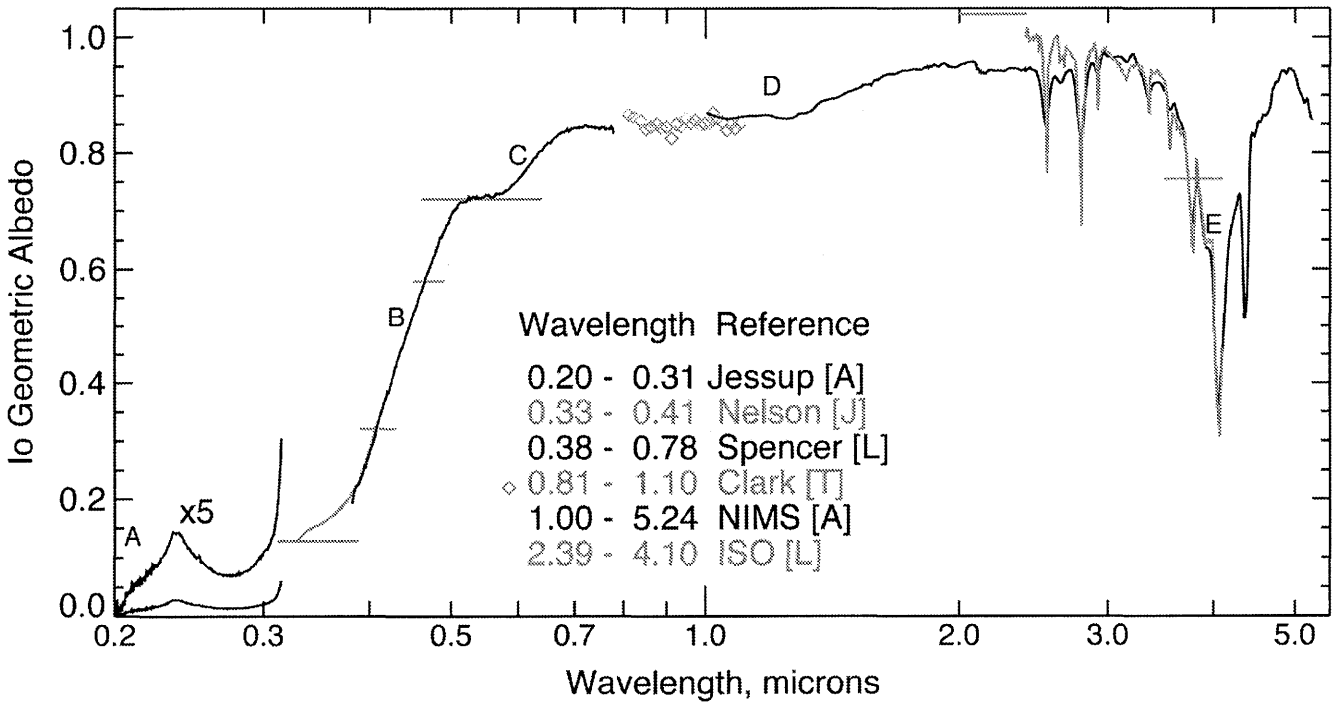

Figure A1.4. Io reflectance spectrum. Spectral identifications: A = SO_2 gas (fine structure below 0.23 μm); B = S_8 or S_nO; C = S_4; D = unknown; E = Cl_2SO_2 (?). Other features are due to SO_2 frost. References: Jessup *et al.* (2002), Nelson and Hapke (1978), Spencer *et al.* (1995), Clark and Mc Cord (1980); NIMS: Carlson *et al.* (1997); ISO: Schmitt *et al.* (2003).

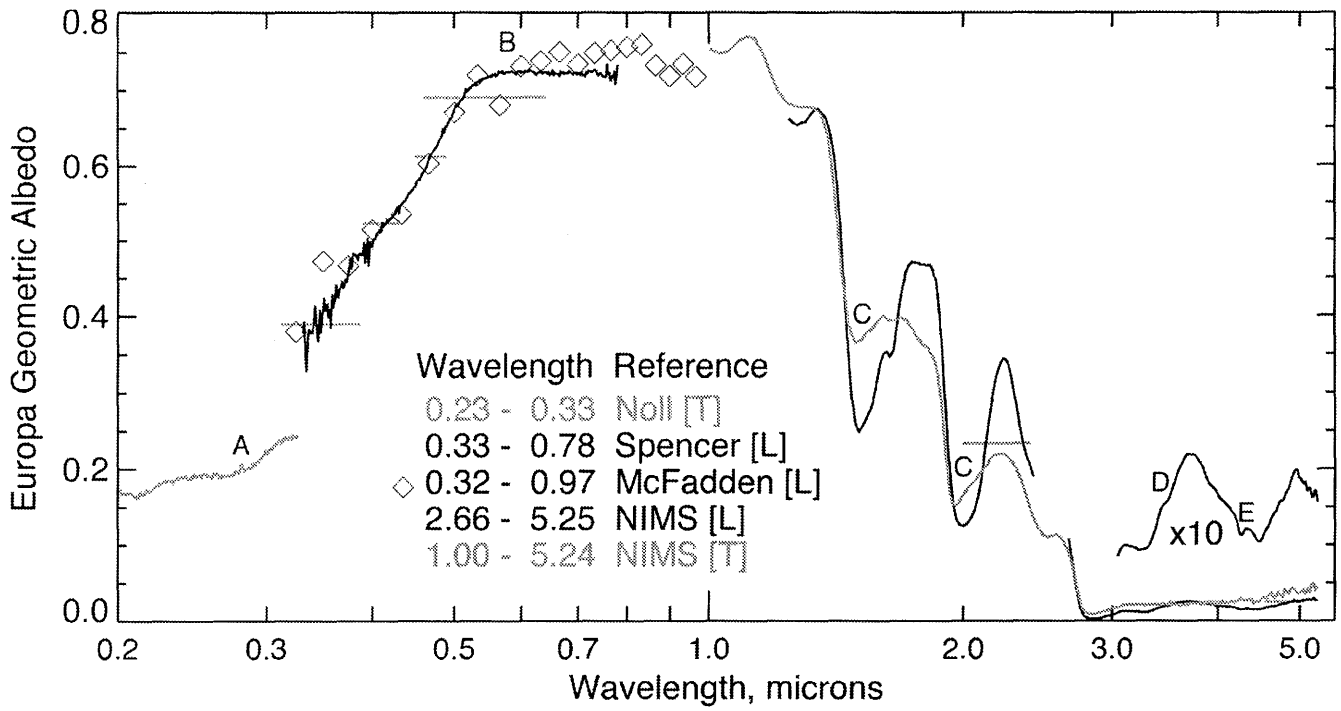

Figure A1.5. Europa reflectance spectrum. See the text for spectral identifications. References: Noll *et al.* (1995), Spencer *et al.* (1995), McFadden *et al.* (1980). NIMS trailing side: 225–270° W, 23° S–31° N, observation "G1 HiLat 01a". NIMS leading side: 120–156° W, 70° S–70° N, observation "E11 1hr 01b". McCord *et al.* (1998).

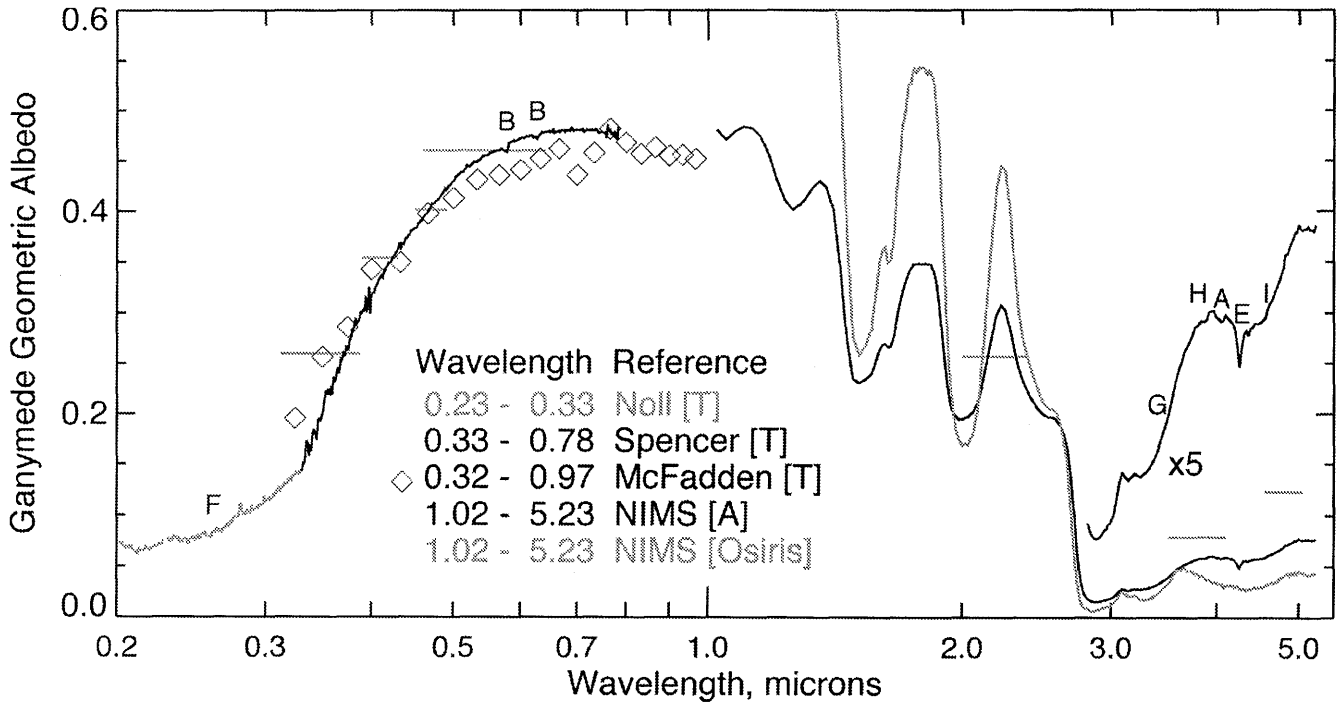

Figure A1.6. Ganymede reflectance spectrum. See the text for spectral identifications. References: Noll *et al.* (1996), Spencer *et al.* (1995), McFadden *et al.* (1980). NIMS anti-Jupiter side: Disk average, observation "G1 Global". NIMS spectrum of the bright icy crater Osiris: 166° W, 38° S, observation "G1 Global". Carlson *et al.* (1996), McCord *et al.* (1998).

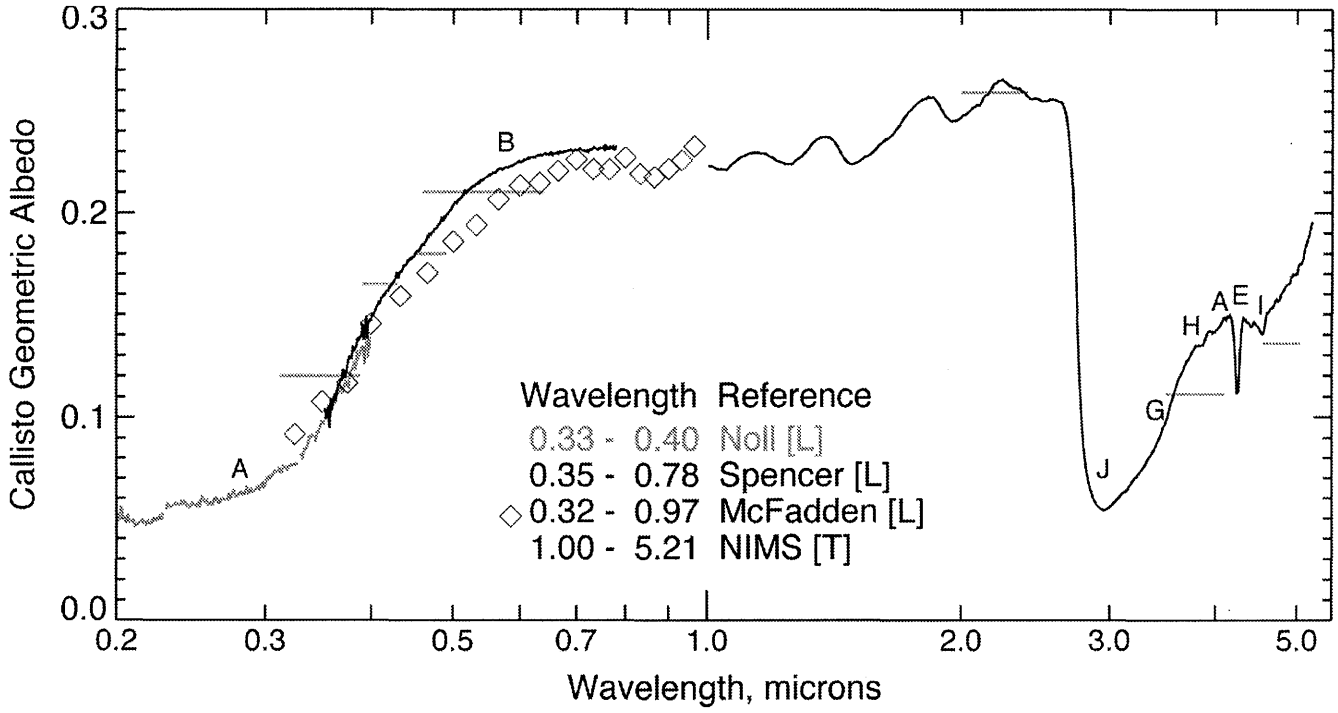

Figure A1.7. Callisto reflectance spectrum. See the text for spectral identifications. References: Noll *et al.* (1997), Spencer *et al.* (1995), McFadden *et al.* (1980). NIMS: 309–332° W, 15° S–20° N, observation "G2CNGLOBAL". McCord *et al.* (1998).

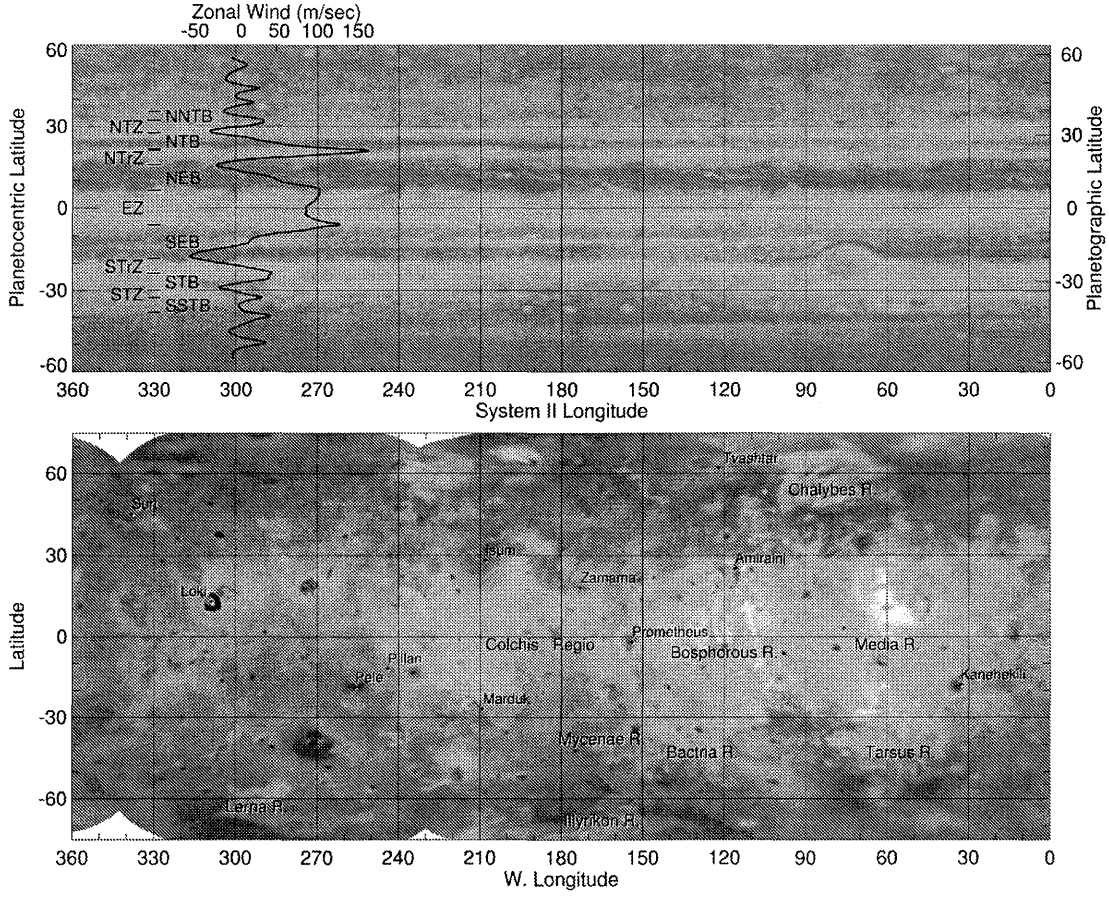

Figure A1.8. TOP: Natural-color cylindrical mosaic of Jupiter based on *Cassini* images taken on October 31, 2000. Scale: 10° of latitude corresponds to 12 500 km at the equator. BOTTOM: Io map. Scale: 10° of latitude corresponds to 318 km. At the time of going to press a colour version of this figure was available for download from http://www.cambridge.org/9780521035453.

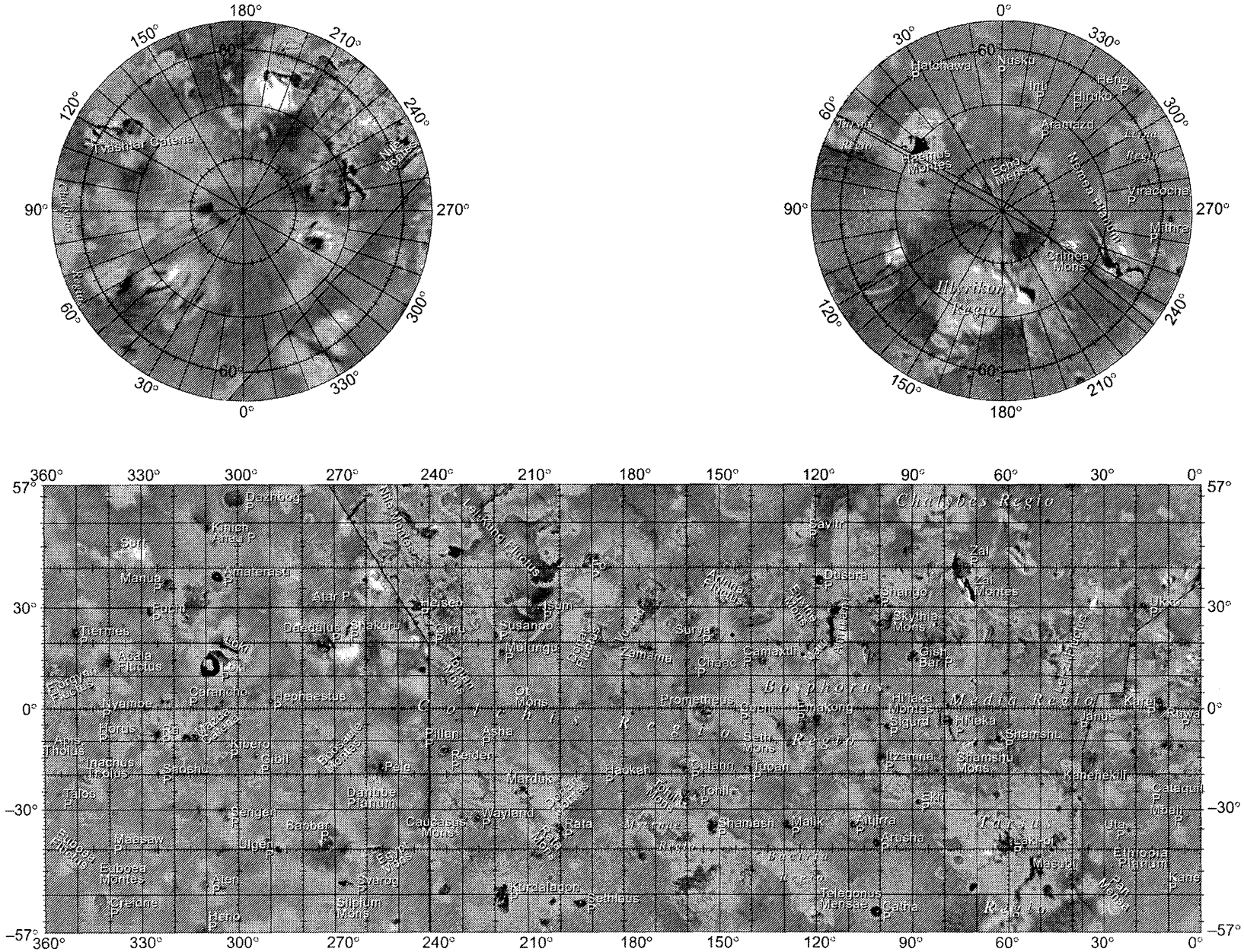

Figure A1.9. Io map. High resolution coverage is emphasized: for lower-resolution color coverage see Fig. A1.8. Based on Fig. 1 of McEwen *et al.* (1998), which shows Io's appearance in 1996 and 1997, with the substitution of a mosaic of 1979 *Voyager 1* images in those regions, centered near longitude 320°, where *Voyager 1* resolution exceeds that of *Galileo*. A black line separates *Voyager* and *Galileo* coverage. In the feature names, "P" stands for "Patera". 10° of latitude on Io corresponds to 318 km.

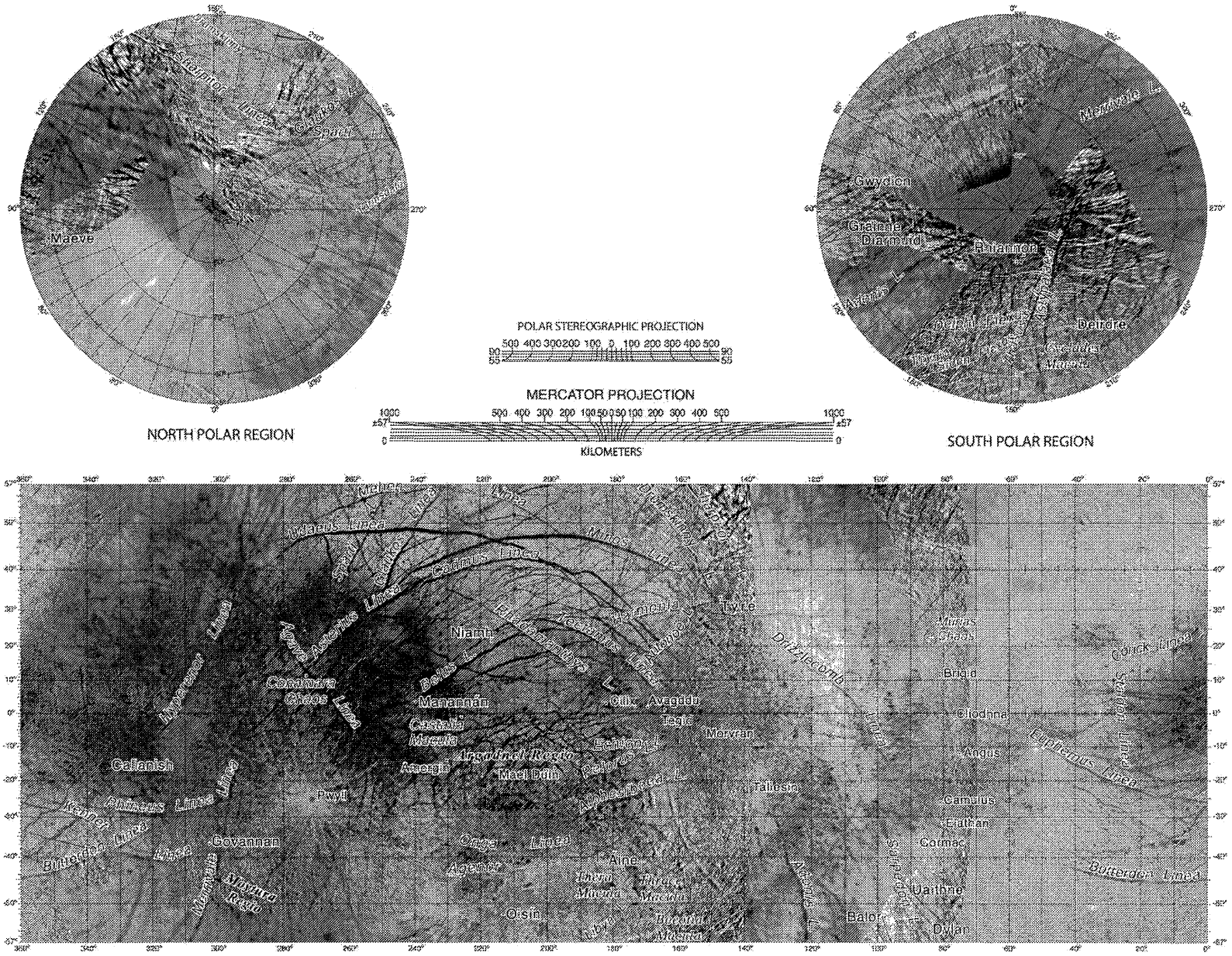

Figure A1.10. Europa map. In the feature names, "L." stand for "Linea". Scale: 10° of latitude corresponds to 273 km.

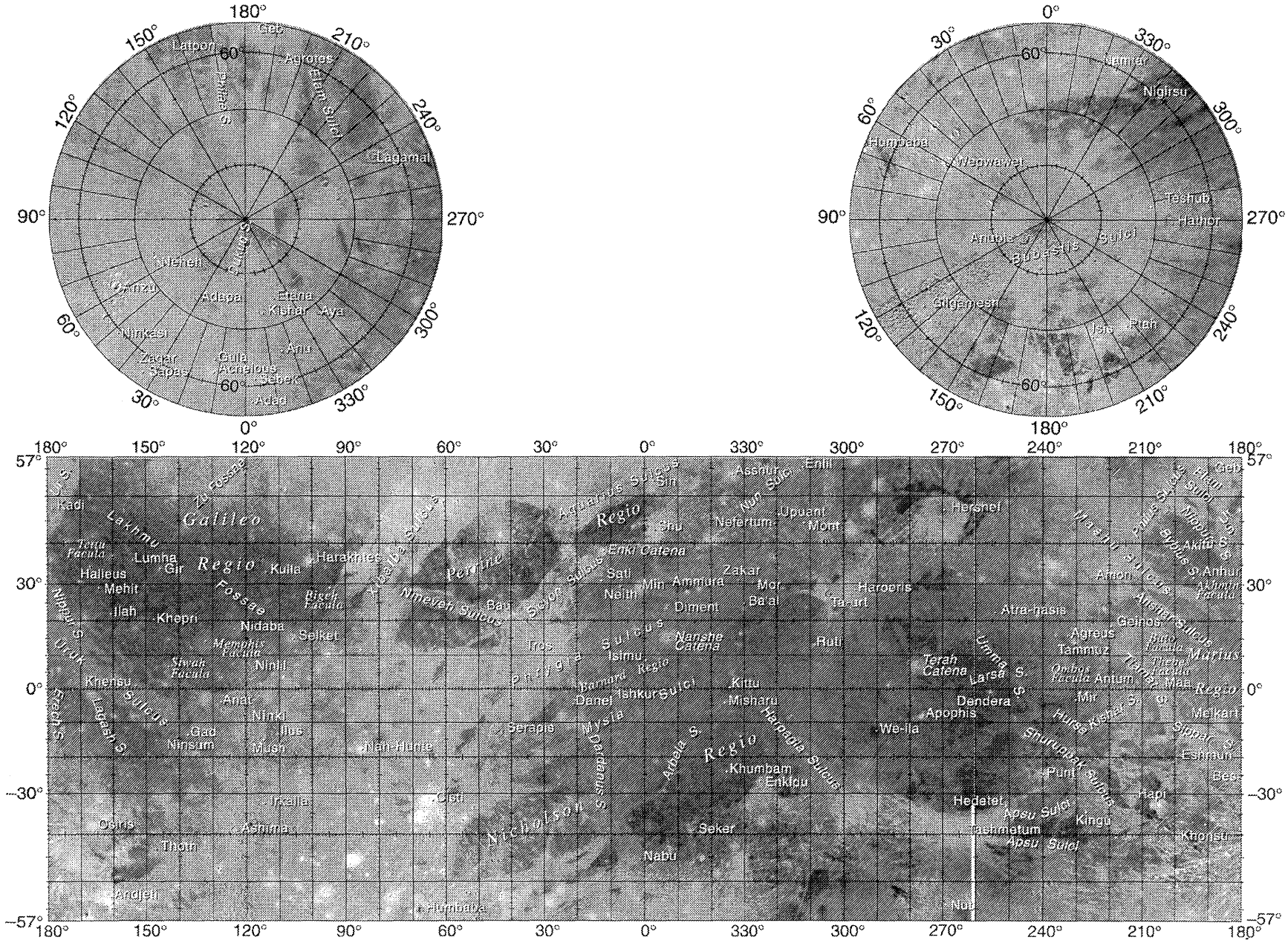

Figure A1.11. Ganymede map. In the feature names, “S.” stands for “Sulcus”. Scale: 10° of latitude corresponds to 460 km.

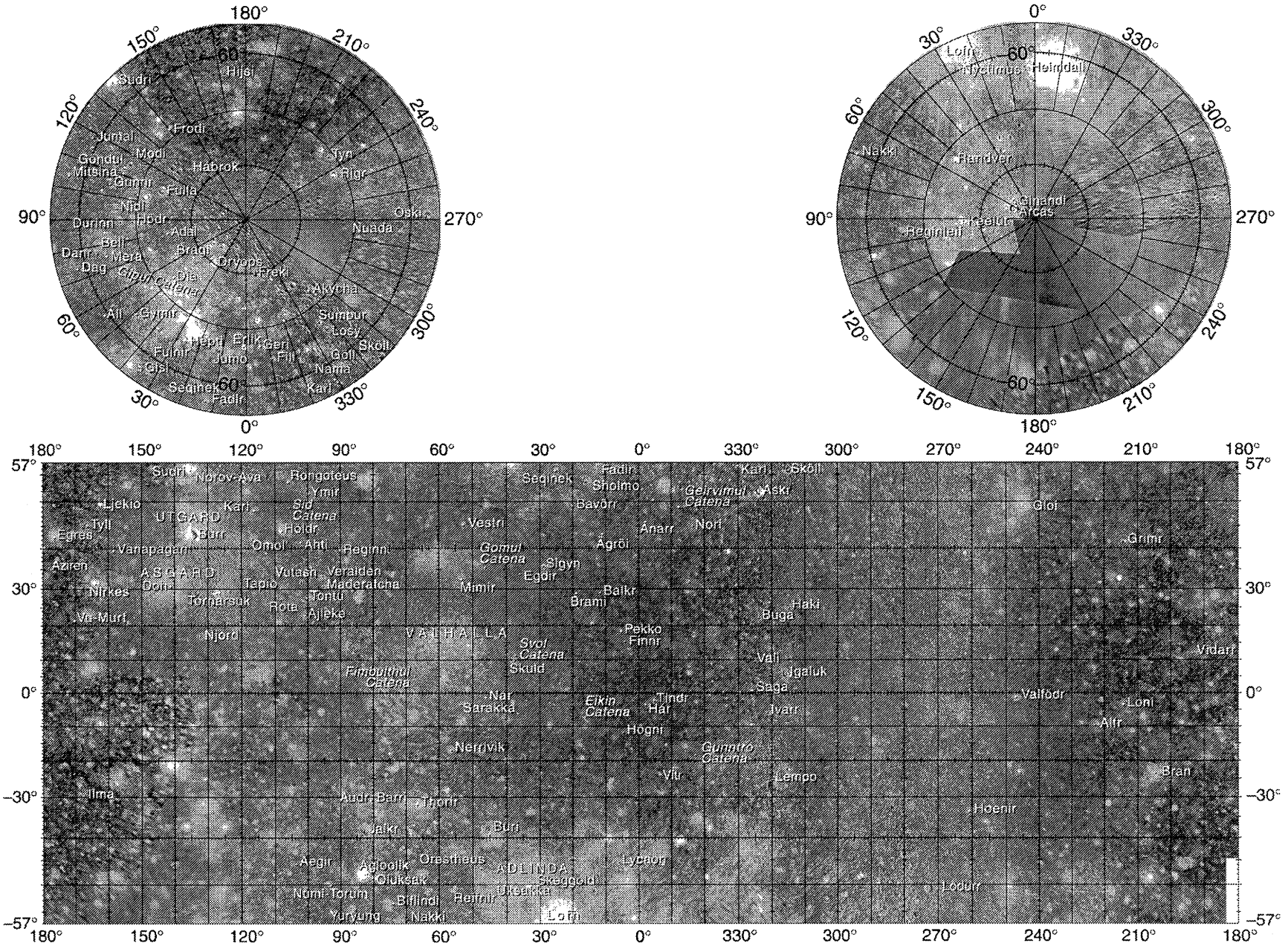

Figure A1.12. Callisto map. Scale: 10° of latitude corresponds to 419 km.

REFERENCES

Bowell, E., B. Hapke, D. Domingue, K. Lumme, J. Peltoniemi, and A. W. Harris, Application of photometric models to asteroids, in *Asteroids II*, R. P. Binzel, T. Gehrels, M. S. Matthews (eds), University of Arizona Press, pp. 524–556, 1989.

Carlson, R., W. Smythe, K. Baines, E. Barbinis, K. Becker, R. Burns, S. Calcutt, W. Calvin, R. Clark, G. Danielson, A. Davies, P. Drossart, T. Encrenaz, F. Fanale, J. Granahan, G. Hansen, P. Herrera, C. Hibbitts, J. Hui, P. Irwin, T. Johnson, L. Kamp, H. Kieffer, F. Leader, E. Lellouch, R. Lopes-Gautier, D. Matson, T. McCord, R. Mehlman, A. Ocampo, G. Orton, M. Roos-Serote, M. Segura, J. Shirley, L. Soderblom, A. Stevenson, F. Taylor, J. Torson, A. Weir, and P. Weissman, Near-infrared spectroscopy and spectral mapping of Jupiter and the Galilean satellites: Results from *Galileo*'s initial orbit, *Science* **274**, 385–388, 1996.

Carlson, R. W., W. D. Smythe, R. M. C. Lopes-Gautier, A. G. Davies, L. W. Kamp, J. A. Mosher, L. A. Soderblom, F. E. Leader, R. Mehlman, R. N. Clark, and F. P. Fanale, Distribution of sulfur dioxide and other infrared absorbers on the surface of Io, *Geophys. Res. Lett.* **24**, 2479, 1997.

Clark, R. N. and T. B. Mc Cord, The Galilean satellites: New near-infrared spectral reflectance measurements (0.65–2.5 microns) and a 0.325–5 micron summary, *Icarus* **41**, 323–339, 1980.

Edgington, S. G., S. K. Atreya, L. M. Trafton, J. J. Caldwell, R. F. Beebe, A. A. Simon, R. A. West, and C. Barnet, On the latitude variation of ammonia, acetylene, and phosphine altitude profiles on Jupiter from HST Faint Object Spectrograph observations, *Icarus* **133**, 192–209, 1998.

Edgington, S. G., S. K. Atreya, L. M. Trafton, J. J. Caldwell, R. F. Beebe, A. A. Simon, and R. A. West, Ammonia and eddy mixing variations in the upper troposphere of Jupiter from HST Faint Object Spectrograph observations, *Icarus* **142**, 342–356, 1999.

Encrenaz, T., T. de Graauw, S. Schaeidt, E. Lellouch, H. Feuchtgruber, D. A. Beintema, B. Bezard, P. Drossart, M. Griffin, A. Heras, M. Kessler, K. Leech, P. Morris, P. R. Roelfsema, M. Roos-Serote, A. Salama, B. Vandenbussche, E. A. Valentijn, G. R. Davis, and D. A. Naylor, First results of ISO-SWS observations of Jupiter, *A&A* **315**, L397–L400, 1996.

Encrenaz, T., P. Drossart, H. Feuchtgruber, E. Lellouch, B. Bézard, T. Fouchet, and S. K. Atreya, The atmospheric composition and structure of Jupiter and Saturn from ISO observations: A preliminary review, *Planet. Space Sci.* **47**, 1225–1242, 1999.

Geissler, P. E., A. S. McEwen, L. Keszthelyi, R. Lopes-Gautier, J. Granahan, and D. P. Simonelli, Global color variations on Io, *Icarus* **140**, 265–282, 1999.

Hanel, R. A., B. J. Conrath, D. E. Jennings, and R. E. Samuelson, *Exploration of the solar system by Infrared Remote Sensing* (2nd Ed.), Cambridge University Press, 2003.

Jessup, K. L., J. Spencer, G. E. Ballester, R. Yelle, F. Roessler, and R. Howell, Spatially resolved UV spectra of Io's Prometheus plume and anti-jovian hemisphere, *BAAS* **34**, 2002.

Karkoschka, E., Methane, ammonia, and temperature measurements of the jovian planets and Titan from CCD-spectrophotometry, *Icarus* **133**, 134–146, 1998.

Khanna, R. K., J. C. Pearl, and R. Dahmani, Infrared spectra and structure of solid phases of sulfur trioxide: Possible identification of solid SO_3 on Io's surface, *Icarus* **115**, 250–257, 1995.

Limaye, S. S., Jupiter: New estimates of the mean zonal flow at the cloud level, *Icarus* **65**, 335–352, 1986.

McCord, T. B., G. B. Hansen, R. N. Clark, P. D. Martin, C. A. Hibbitts, F. P. Fanale, J. C. Granahan, M. Segura, D. L. Matson, T. V. Johnson, R. W. Carlson, W. D. Smythe, and G. E. Danielson, Non-water-ice constituents in the surface material of the icy Galilean satellites from the *Galileo* Near-Infrared Mapping Spectrometer investigation, *J. Geophys. Res.* **103**, 8603–8626, 1998.

McEwen, A. S., L. Keszthelyi, P. Geissler, D. P. Simonelli, M. H. Carr, T. V. Johnson, K. P. Klaasen, H. H. Breneman, T. J. Jones, J. M. Kaufman, K. P. Magee, D. A. Senske, M. J. S. Belton, and G. Schubert, Active volcanism on Io as seen by *Galileo* SSI, *Icarus* **135**, 181–219, 1998.

McFadden, L. A., J. F. Bell, and T. B. McCord, Visible spectral reflectance measurements (0.33–1.1 microns) of the Galilean satellites at many orbital phase angles, *Icarus* **44**, 410–430, 1980.

Mills, F. P. and M. E. Brown, Thermal infrared spectroscopy of Europa and Callisto, *J. Geophys. Res.* **105**, 15 051–15 060, 2000.

Morrison, D. and N. D. Morrison, Photometry of the Galilean satellites, in *Planetary Satellites*, J. A. Burns (ed), University of Arizona Press, pp. 363–378, 1977.

Nelson, R. M. and W. Hapke, Spectral reflectivities of the Galilean satellites and Titan: 0.32 to 0.86 micrometers, *Icarus* **36**, 304–329, 1978.

Noll, K. S., H. A. Weaver, and A. M. Gonnella, The albedo spectrum of Europa from 2200 Å to 3300 Å, *J. Geophys. Res.* **100**, 19 057–19 060, 1995.

Noll, K. S., R. E. Johnson, A. L. Lane, D. L. Domingue, and H. A. Weaver, Detection of ozone on Ganymede, *Science* **273**, 341, 1996.

Noll, K. S., R. E. Johnson, M. A. McGrath, and J. J. Caldwell, Detection of SO_2 on Callisto with the Hubble Space Telescope, *Geophys. Res. Lett.* **24**, 1139, 1997.

Porco, C. C., R. A. West, A. McEwen, A. D. Del Genio, A. P. Ingersoll, P. Thomas, S. Squyres, L. Dones, C. D. Murray, T. V. Johnson, J. A. Burns, A. Brahic, G. Neukum, J. Veverka, J. M. Barbara, T. Denk, M. Evans, J. J. Ferrier, P. Geissler, P. Helfenstein, T. Roatsch, H. Throop, M. Tiscareno, and A. R. Vasavada, *Cassini* imaging of Jupiter's atmosphere, satellites, and rings, *Science* **299**, 1541–1547, 2003.

Rogers, J. H., *The Giant Planet Jupiter*, Cambridge University Press, 1995.

Schmitt, B., E. Lellouch, S. Douté, C. Feuchtgruber, C. De Bergh, and J. Crovisier, High resolution infrared spectra (2.4–5.3 μm) of the surface of Io with ISO: The physical state of solid SO_2, *J. Geophys. Res.* **in preparation**, 2003.

Spencer, J. R., *The Surfaces of Europa, Ganymede, and Callisto: An Investigation using* Voyager *IRIS Thermal Infrared Spectra*, Ph.D. thesis, University of Arizona, 1987.

Spencer, J. R., W. M. Calvin, and M. J. Person, CCD spectra of the Galilean satellites: Molecular oxygen on Ganymede, *J. Geophys. Res.* **100**, 19 049–19 056, 1995.

Tittemore, W. C. and W. M. Sinton, Near-infrared photometry of the Galilean satellites, *Icarus* **77**, 82–97, 1989.